BOREAL ENVIRONMENT RESEARCH 16 (suppl. A): 15–26
ISSN 1239-6095 (print) ISSN 1797-2469 (online)

Helsinki 31 March 2011

Simulation of mesoscale structures and nutrient transport during summer upwelling events in the Gulf of Finland in 2006

Jaan Laanemets[1)], Germo Väli[1)], Victor Zhurbas[1)2)], Jüri Elken[1)], Inga Lips[1)] and Urmas Lips[1)]

[1)] *Marine Systems Institute, Tallinn University of Technology, Akadeemia tee 21, Tallinn 12618, Estonia*
[2)] *Shirshov Institute of Oceanology, 36 Nakhimovsky Prospect, Moscow 117851, Russia*

Received 30 Oct. 2009, accepted 15 Apr. 2010 (Editor in charge of this article: Kai Myrberg)

Laanemets, J., Väli, G., Zhurbas, V., Elken, J., Lips, I. & Lips, U. 2011: Simulation of mesoscale structures and nutrient transport during summer upwelling events in the Gulf of Finland in 2006. *Boreal Env. Res.* 16 (suppl. A): 15–26.

A high resolution numerical study was carried out to simulate a series of upwelling events and related nutrient transport in the Gulf of Finland. In order to characterize the intensity of water motions of different nature in the surface layer, simulated velocity components were decomposed into mesoscale fluctuations, inertial oscillations and mean currents. Mean currents contained 14%, inertial oscillations 20% and mesoscale fluctuations 66% of the total kinetic energy. High values of kinetic energy of mesoscale fluctuations were in the coastal zones (up to 0.03 m^2 s^{-2}) due to along-shore baroclinic upwelling/downwelling jets and in the narrowest western-central part (0.01–0.02 m^2 s^{-2}) of the Gulf, where intensive squirts and eddies were formed. In this region also the most intensive coastal offshore exchange of upwelled nutrients occurred. The total content of phosphorus and nitrogen in the upper 10-m layer introduced by the upwelling events was estimated at 1100 tonnes, with a clear excess of phosphorus.

Introduction

Upwelling is a typical phenomenon in the Baltic Sea, redistributing both the heat and salt in coastal regions and replenishing the surface layer with nutrients, especially in summer when the surface layer is depleted of nutrients. Model simulations have shown that the annual-averaged frequency of strong upwelling may be as high as 30% in some parts of the Baltic Sea (Kowalewski and Ostrowski 2005). Owing to the prevailing south-westerly winds (e.g. Soomere and Keevallik 2003) the northern part of the Gulf of Finland is an active upwelling area as shown by satellite sea surface temperature data (e.g. Kahru *et al*. 1995, Uiboupin and Laanemets 2009) and model simulations (Myrberg and Andrejev 2003). According to field data, summer upwelling events usually transport nutrients with the excess of phosphorus in relation to the Redfield ratio into the surface layer in the Gulf of Finland (Haapala 1994, Kononen *et al*. 2003, Vahtera *et al*. 2005, Lips *et al*. 2009). The excess phosphorus input is most likely a result of low nitrogen to phosphorus ratio in the deeper layers of the Gulf (Lehtoranta 2003) and the higher depth of phosphacline than nitracline in the range of thermocline (Laanemets *et al*. 2004). Model experiments by Laanemets *et al*. (2009) showed that a different ability of upwelling along the

northern and southern coast to transport nutrients to the surface layer is caused by the features of bottom topography. A steeper bottom slope and greater sea depths along the southern coast caused larger nutrient inputs under the same magnitude of wind forcing. An important aspect related to the nutrient enrichment of the whole Gulf surface layer by upwelling is an enhanced coastal offshore exchange during the relaxation phase. Model simulations by Zhurbas *et al*. (2008) showed that the instability of along-shore baroclinic jets and related thermohaline fronts caused by coupled upwelling and downwelling events lead to the development of filaments/squirts remarkably increasing the lateral eddy diffusivity.

A comprehensive review of the Baltic Sea upwelling, its dynamics and reflections to ecosystem is presented by Lehmann and Myrberg (2008) and Myrberg *et al*. (2008).

Summer 2006 was characterized by quite a rare meteorological situation — easterly winds that are favourable for the upwelling along the southern coast of the Gulf prevailed during a relatively long period (whole August). As a result, a very intensive upwelling was observed along the southern coast (Lips *et al*. 2009). During 2000–2006, it was the largest upwelling by area on the southern coast [20% of the total Gulf area; Uiboupin and Laanemets (2009)]. The cross-shore extent of the upwelling zone amounted to 25 km (about 1/3 of the Gulf's width) and the along-shore extent up to 360 km (Suursaar and Aps 2007). Water temperature along the southern coast was as low as 5–8 °C for about two weeks (based on the unpublished data of operational measurements from the TUT Marine Systems Institute and the Estonian Meteorological and Hydrological Institute) while the offshore temperature was in a range 18–22 °C (Lips *et al*. 2008).

The present paper is aimed to investigate a sequence of upwelling events including intensive upwelling along the southern coast of the Gulf in July–August 2006, combining the results of model simulations with these of the field measurements and satellite imagery. The objectives are (1) to simulate mesoscale variability of temperature, velocity and nutrients fields, (2) to characterize the intensity of water motions of different nature (mesoscale fluctuations, inertial oscillations, and mean currents) in the surface layer, (3) to estimate total inputs and averaged spatial distributions of nutrients caused by a sequence of upwelling events.

Model setup

We applied the Princeton Ocean Model (POM) (Blumberg and Mellor 1983) in the Baltic Sea. The POM is a primitive equation, sigma coordinate, free surface, hydrostatic model with a second moment turbulent closure sub-model embedded. The horizontal step of the model grid is 0.5 nautical miles in the Gulf (Fig. 1) and reaches 2 nautical miles in the rest of the Baltic Sea; there are 30 σ-levels in the vertical direction. The digital topography of the sea bottom is taken from Seifert and Kayser (1995). The refinement of the bottom topography in the Gulf was done by means of bilinear interpolation of the original 1.0 nautical-mile grid. A model resolution of 0.5 nautical miles allows resolving mesoscale phenomena, including upwelling filaments/squirts (Zhurbas *et al*. 2008) controlled by the internal baroclinic Rossby radius the value of which varies within 2–5 km in the Gulf (Alenius *et al*. 2003).

Model simulations were carried out from 10 July to 31 August 2006 covering several upwelling events along both the northern and the southern coasts of the Gulf, including a very intense upwelling event along the southern coast during the first half of August. Atmospheric forcing (wind stress and surface heat flux components) was calculated from wind, solar radiation, air temperature, total cloudiness and relative humidity data taken from HIRLAM (High Resolution Limited Area Model) version of the Estonian Meteorological and Hydrological Institute with the spatial resolution of 11 km and forecast interval of 1 h ahead of 54 h, recalculated after every 6 h (Männik and Merilain 2007). Wind velocity components at the 10-m level along with the other HIRLAM meteorological parameters were interpolated to the model grid. The model domain is closed at the Danish straits by an artificial shore since during the simulation period the spatially mean Baltic Sea

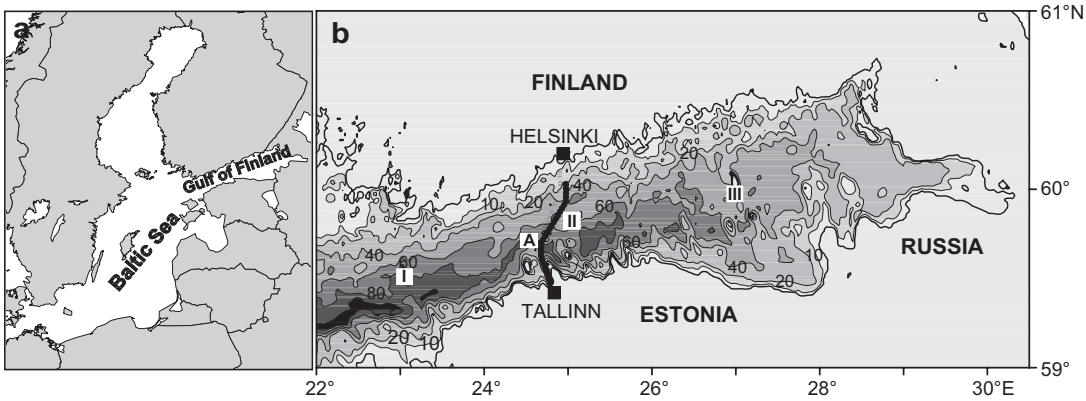

Fig. 1. (**a**) A map of the Baltic Sea, and (**b**) a close-up of the Gulf of Finland, where the model grid is refined to 0.5 nautical miles. Location of the transect (thick line) of nutrient sampling stations between Tallinn and Helsinki; the time series of HIRLAM wind data in the (I) western, (II) central and (III) eastern Gulf; and (A) a temporal snapshot of a simulated vertical distribution of the *u* component of velocity, phosphate and NO_x concentrations are shown. The depths are given in meters.

level was very stable: by our estimates from the open boundary model, the variations were less than 0.05 m, while the long-term variations of the mean sea level of the Baltic may exceed 1 m (Lehmann *et al*. 2004). Freshwater supply, although of secondary importance for the upwelling dynamics, was applied as the Neva river inflow with the volume rate of 77.6 km^3 yr^{-1} (Bergström *et al*. 2001).

Initial thermohaline fields were taken from HIROMB (High Resolution Operational Model of the Baltic Sea), a *z*-level model, from the 1 nautical mile grid step version as provided by SMHI (Funkquist 2001). The vertical grid step is 4 m in the surface layer down to 12 m and increases towards greater depths, resulting in 16 layers at 230 m. Thermohaline fields of HIROMB were first interpolated to our horizontal model grid and before the transformation from *z*-levels to σ-levels were smoothed horizontally with averaging length of 10 nautical miles in the Gulf. The latter procedure was necessary to suppress the dynamical imbalances of mesoscale motions that may occur during the grid conversion. In upwelling-dominated situations, POM is able to reproduce mesoscale variability of upwelling in the Gulf, including filaments/squirts and eddies, starting from quite smooth initial thermohaline conditions (Zhurbas *et al*. 2008).

Two equations describing passive tracer balance were introduced to POM to simulate nutrient (phosphate, and nitrate + nitrite henceforth called NO_x) transport. In order to estimate the amount of nutrients transported from deep layers to the upper mixed layer due to upwelling and further lateral transport by filaments and eddies, nutrients were considered as conservative passive tracers. This approach does not include the effects of biogeochemical processes the contribution of which to the time rate of the change of nutrients is small during intensive upwelling (Tilstone *et al*. 2000). The equations were solved numerically within the POM code in the same way as those for temperature and salinity. In order to describe the initial fields of nutrients, we used the data collected along a repeated transect of 14 stations on the line Tallinn–Helsinki on 11 and 25 July 2006 (Fig. 1); the distance between sampling stations was 5.2 km; the samples were collected mainly from the 0–40-m layer (Lips *et al*. 2009). Vertical resolution in the thermocline layer was 2.5–5 m and one sample was taken from the near-bottom layer. In the upper mixed layer, nutrient concentrations were below or close to the detection level and in the model, the initial fields were therefore set to zero in this layer. According to the measurements the nutriclines were tightly coupled with the thermocline and slightly separated, the phosphacline situated at shallower depths (*see* Lips *et al*. 2009). We, therefore, introduced linear profiles for PO_4 and NO_x concentrations between the depth of a certain isothermal surface in the thermocline and

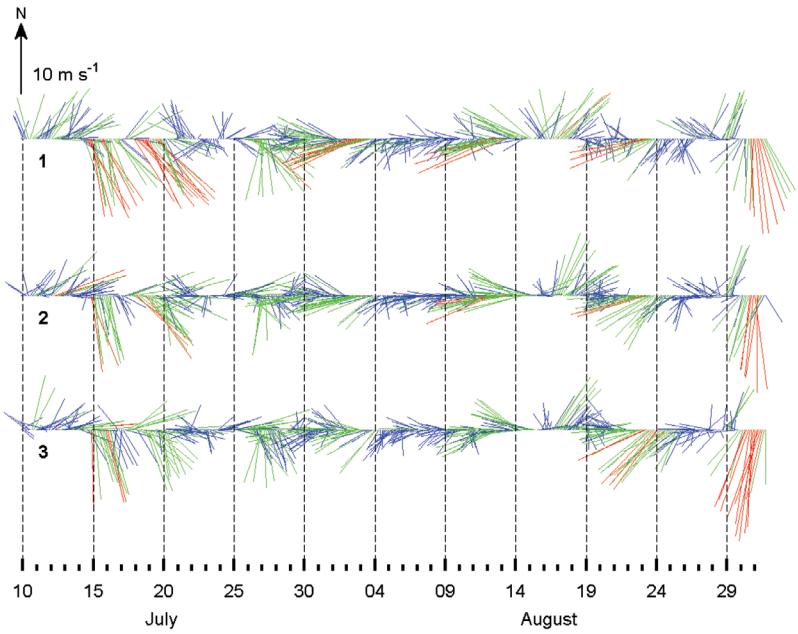

Fig. 2. Time series of the 10-m level HIRLAM wind vector in the (1) western, (2) central and (3) eastern parts of the Gulf of Finland for the period 10 July–31 August, 2006. Colours: blue = wind speed < 6 m s^{-1}, green = 6 ≤ wind speed ≤ 10 m s^{-1}, red = wind speed > 10 m s^{-1}.

the 40-m depth. The best fit was obtained when isothermal surfaces of 7 and 11 °C as upper locations of nitracline and phosphacline, and PO_4 and NO_x concentrations at the 40-m depth of 0.6 and 1.7 mmol m^{-3} were used, respectively. We extended nutrient profiles to a greater depth using the data from other sources (Zhurbas *et al*. 2008). The assembled vertical distributions of nutrient concentrations are

$$PO_4 = \begin{cases} 0, & 0 \le z \le h_{11°C} \\ 0.6\left(z - h_{11°C}\right) \Big/ \left(40 - h_{11°C}\right), & h_{11°C} < z \le 40 \text{ m} \\ 0.013\left(z - 40\right) + 0.6, & z > 40 \text{ m} \end{cases}$$

$$NO_x = \begin{cases} 0, & 0 \le z \le h_{7°C} \\ 1.7\left(z - h_{7°C}\right) \Big/ \left(40 - h_{7°C}\right), & h_{7°C} < z \le 40 \text{ m} \\ 0.066\left(z - 40\right) + 1.7, & z > 40 \text{ m} \end{cases} \quad (1)$$

where z is the depth in meters, $h_{11°C}$ and $h_{7°C}$ are the depths of 11 °C and 7 °C isothermal surfaces in the model initial data, respectively. The vertical profiles of nutrients described above were extended to the whole Baltic Sea. This procedure excludes the effects of horizontal nutrient fluxes, which do exist due to the horizontal gradients of nutrient concentrations (in summer below the euphotic zone). There are large horizontal gradients of nutrients in the Gulf of Finland (e.g. Kuuppo *et al*. 2006: fig. 5). However, the approach we used allows us better to single out the effects of vertical nutrient fluxes.

The model runs from the motionless state and zero surface elevation starting at 00:00 of 10 July 2006.

Results and discussion

Modelled upwelling dynamics

Depending on the ability to drive upwelling, the overall simulation period can be divided into two parts: a relatively short westerly-component wind period (before 29 July) followed by a long-lasting easterly-component wind period (after 31 July) (Fig. 2). The easterly (westerly) component winds are favourable for upwelling along the southern (northern) coast of the Gulf. There were four time intervals when the speed of the wind favourable for upwelling near the southern coast exceeded 10 m s^{-1} (on 3, 13, 23, and 30 August). Within this easterly wind period there was a 3-day interval of reverse, south-westerly wind (from 16 to 18 August) which would result in a temporary weakening of upwelling (i.e., the decrease of cold water temperature contrast) along the southern coast or would even produce upwelling along the opposite, northern coast.

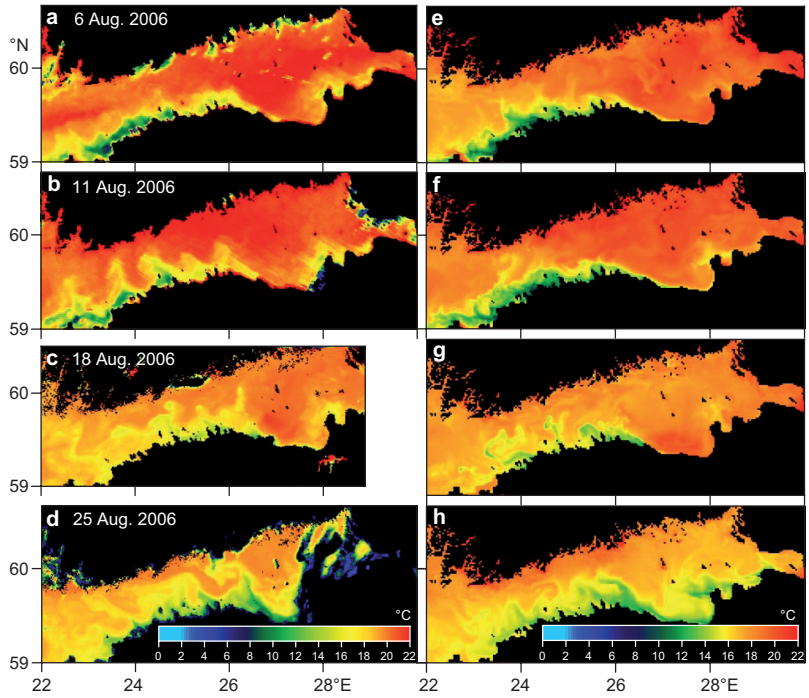

Fig. 3. SST maps of the Gulf of Finland in August 2006: (**a–d**) satellite imagery and (**e–h**) simulations.

The real effect of the reverse wind will be discussed later in this section.

A comparison of SST maps obtained from satellite imagery within the period of upwelling along the southern coast of the Gulf with that of simulations (Fig. 3) indicates that:

1. on 6 and 11 August, the most intensive upwelling along the southern coast is observed in the western part of the Gulf,
2. on 25 August the intensive upwelling area shifted to the eastern part of the Gulf. The displacement of the upwelling area occurred due to spatial changes in the wind field: the speed of E–SE winds on 25 August (6 and 11 August) was higher in the eastern (western) part of the Gulf (*see* Fig. 2),
3. on 18 August the intensity of upwelling was weakened due to transient SW winds (*see* Fig. 2),
4. the characteristic features of mesoscale coherent structures (i.e. filaments/squirts) observed in the satellite SST maps were reasonably well reproduced by simulations. Of course it does not mean the identity of individual mesoscale structures.

A simulated mesoscale variability of the surface layer currents in the course of upwelling/downwelling events is illustrated in Fig. 4. In order to eliminate inertial oscillations, which are able to mask 'pure' mesoscale motions, the former were filtered out using a simple procedure:

$$\tilde{\boldsymbol{v}}(\boldsymbol{x},t) = 0.5\boldsymbol{v}(\boldsymbol{x},t) + 0.25\left[\boldsymbol{v}\left(\boldsymbol{x},t-\frac{T_i}{2}\right)+\boldsymbol{v}\left(\boldsymbol{x},t+\frac{T_i}{2}\right)\right], \quad (2)$$

where $\boldsymbol{v}(\boldsymbol{x},t)$ and $\tilde{\boldsymbol{v}}(\boldsymbol{x},t)$ are the velocity vectors at the 2-m depth before and after the filtration, respectively, $T_i \equiv 2\pi/f = 0.58$ day is the inertia oscillation period, f is the Coriolis parameter. Upwelling along the north coast of the Gulf (Fig. 4a) is characterized by transverse cold water filaments and related to transverse jet-like currents or squirts with southward velocities up to 0.3 m s^{-1}. Some of the squirts penetrate almost the whole width of the Gulf.

The culmination of upwelling along the southern coast of the Gulf is shown in Fig. 4b. The pattern of cold water transverse filaments and squirts developed from the upwelling along

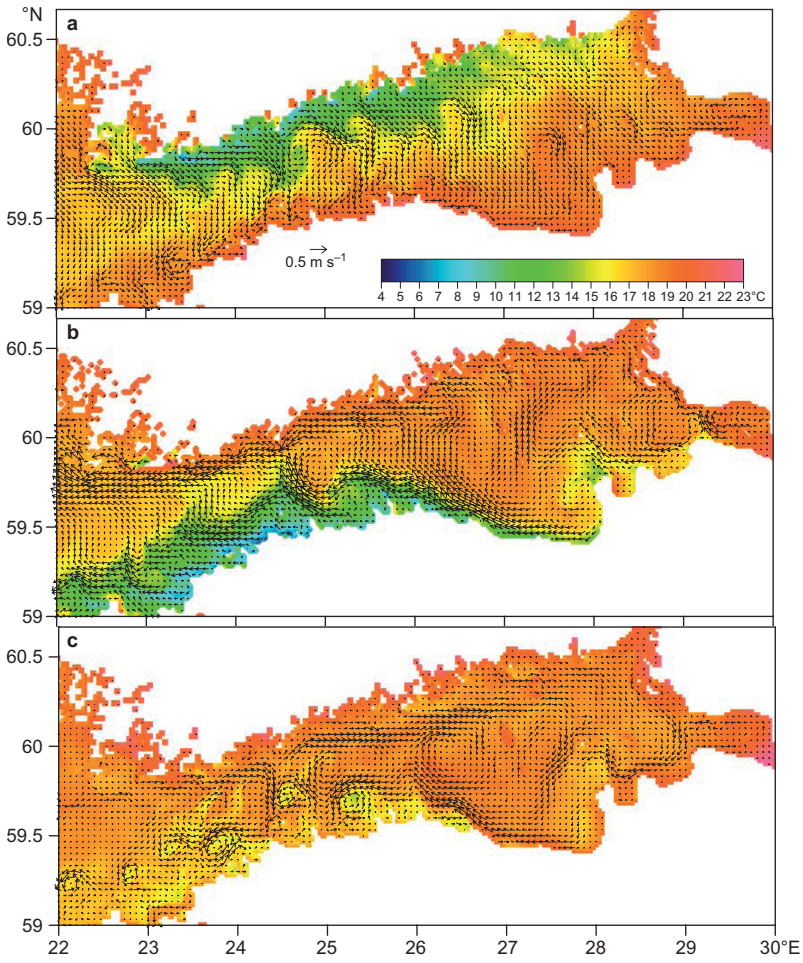

Fig, 4. Simulated surface layer currents (vectors) and SST in the Gulf in the course of upwelling/downwelling events on (**a**) 26 July (01:00 UTC), (**b**) 13 August (17:00 UTC), and (**c**) 19 August (18:15 UTC). The vectors of current are depicted in every fourth grid nodes.

the southern coast to some extent looks like a mirror image of the upwelling along the northern coast (cf. Fig. 4a and b). The most intensive cold water filament and squirt with northward velocity up to 0.4 m s^{-1} was observed at the narrowest part of the Gulf between Tallinn and Helsinki. Note that the along-shore distribution of transverse filaments and squirts related to the upwelling along the southern coast is less uniform than that of the northern coast likely because the southern coast of the Gulf is curved while the northern coast is relatively straight.

Due to the transient reverse of wind direction from east to west, the upwelling along the southern coast weakened (Fig. 4c). A striking feature here is the formation of several mesoscale cyclonic eddies in the southwestern part of the Gulf of Finland: one can discern at least six cyclonic eddies with the diameter of 12–24 km and rotation velocity of 0.2 m s^{-1}. This is just in accordance with Zhurbas *et al*. (2006), who showed that the instability of an upwelling (downwelling) baroclinic jet results in a selective formation of mostly cyclonic (anticyclonic) eddies.

Kinetic energy during upwelling

In order to characterize the intensity of water motions of different nature in the surface layer of the Gulf, the simulated velocity components at the 2-m depth, (u,v) were decomposed into mesoscale (eddy) fluctuations (u'_E, v'_E), inertial oscillations (u'_I, v'_I) and mean currents $(\overline{u}, \overline{v})$

$$u = u'_E + u'_I + \overline{u}, \quad v = v'_E + v'_I + \overline{v}, \qquad (3)$$

where overbar means the time averaging over the whole simulation period. Inertial oscillations were separated using Eq. 2. Then the mean kinetic energy per unit volume was calculated for each type of motions

$$\begin{aligned} \mathrm{EKE} &= \left(\overline{u_{\mathrm{E}}'^2} + \overline{v_{\mathrm{E}}'^2}\right)/2 \\ \mathrm{IKE} &= \left(\overline{u_{\mathrm{I}}'^2} + \overline{v_{\mathrm{I}}'^2}\right)/2 \cdot \\ \mathrm{MKE} &= \left(\overline{u}^2 + \overline{v}^2\right)/2 \end{aligned} \qquad (4)$$

The MKE data are of minor interest because the averaging period (53 days) does not allow MKE interpretation as seasonal or annual means. At the same time, the simulation period of 53 days is long enough to obtain some statistics of mesoscale fluctuations (eddies, squirts) and inertial oscillations and, therefore, to analyze EKE and IKE maps (Fig. 5). The EKE level is the highest (up to 0.03 $m^2\ s^{-2}$) in the coastal zone close to the southern and northern shores of the Gulf where variable wind forcing produces alongshore baroclinic jet currents of alternating direction due to successive upwelling and downwelling events (Fig. 5a). Again, high enough values of EKE (0.01–0.02 $m^2\ s^{-2}$ which corresponds to r.m.s. velocity fluctuations of 0.14–0.20 m s^{-1}) are found in the narrow western and central parts of the Gulf, where intensive transverse squirts and eddies are formed (cf. Figs. 4 and 5a).

In contrast to EKE, the energy of inertial oscillations is relatively uniformly distributed within open waters (IKE ≈ 0.004 $m^2\ s^{-2}$) and decreases below 0.002 $m^2\ s^{-2}$ in coastal and shallow zones (as close as 1–2 nautical miles to the shore and as shallow as 20 m of the sea depth) (Fig. 5b).

The average levels of EKE, IKE and MKE in the surface layer of the Gulf were estimated as <EKE>/<IKE>/<MKE> = 0.0072/0.0021/0.0015 $m^2\ s^{-2}$. In other words, EKE, IKE, and MKE contain 66%, 20% and 14% of the total kinetic energy, respectively.

A cold water filament and a related transverse squirt on the beam of Tallinn Bay being initially wide (*see* Fig. 4b) narrowed and created a bottleneck in the middle to connect with a cyclonically rotating cold water pool in the north (Fig. 6a).

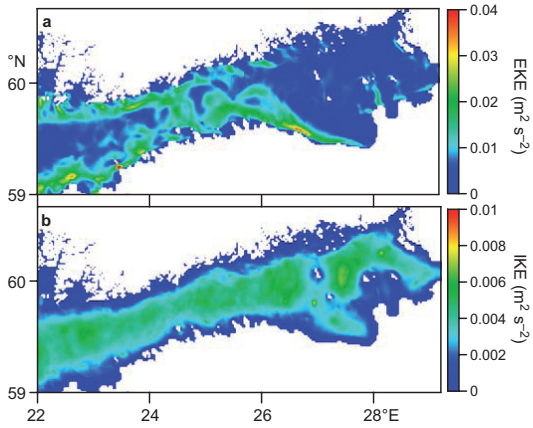

Fig. 5. Maps of simulated (**a**) eddy kinetic energy and (**b**) inertial oscillation kinetic energy in the surface layer of the Gulf.

The bottleneck was expected to vanish in a while, which would mark the accomplishment of cyclonic eddy formation. This cyclonic eddy was clearly identified for more than two days (Fig. 4c). The currents related to the bottleneck and it is likely that also the cyclonic eddy could occupy the upper sea layer that is 20–30 m thick (Fig. 6c).

Nutrient dynamics

The ability of the model to reproduce nutrient transport into the surface layer in the course of upwelling events is demonstrated by comparing the simulated nutrient distribution with a corresponding distribution sampled on a transect between Tallinn and Helsinki (Fig. 7). The model reproduced both the PO_4 and NO_x distributions reasonably well even after about one-month simulation period covering several upwelling events along the northern coast and a strong upwelling event along the southern coast (Fig. 7). The simulated and measured PO_4 concentration values in the upwelling zone (Fig. 7c and d) were approximately the same whereas NO_x concentrations (Fig. 7a and b) differed more. This and the higher simulated NO_x and PO_4 concentrations in the surface layer at the warmer side of the upwelling front can be explained by the lack of nutrient consumption in the model. Also, it is worth mentioning that the observed nutrient

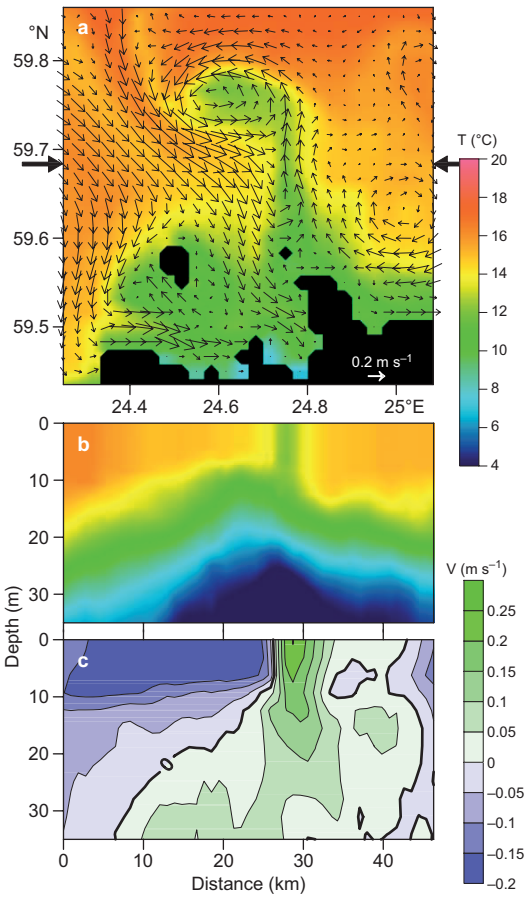

Fig. 6. Snapshot of a simulated cold-water filament and related transverse squirt transforming into a cyclonic eddy. (**a**) SST and surface layer currents off Tallinn Bay on 17 August, 06:45 UTC, (**b**) temperature, and (**c**) *v* component of velocity *vs.* distance and depth on a zonal transect marked by thick arrows. Velocity vectors are depicted in every second grid nodes.

distributions look more patchy than the modelled ones. This is not surprising because the above-described parameterisation of initial nutrient distributions implies strong spatial averaging of data available.

Upwelling along the northern coast of the Gulf is accompanied by downwelling along the southern coast and vice versa. When the wind forcing weakens, the instability of two alongshore baroclinic jets and related fronts of a coupled upwelling/downwelling event produce cold/warm filaments (Fig. 4). The important role of filaments and eddies in the offshore transport and lateral mixing of upwelled nutrients in the Gulf was shown by Zhurbas *et al*. (2008) and Laanemets *et al*. (2009).

In order to evaluate the total nutrient input to the surface layer of the Gulf produced by a series of upwelling events in July–August 2006, the simulated concentrations of phosphorus and nitrogen were integrated in the upper 10-m layer over the whole Gulf area. The longitude 22°E was taken as the western boundary of the Gulf, including the entrance area. The integration depth of 10 m corresponds approximately to the depth of the euphotic zone in the relatively turbid Gulf of Finland (e.g. Kononen *et al*. 2003). Temporal courses of the total content of phosphorus and nitrogen in the surface layer of the Gulf are depicted in Fig. 8.

During the period from 10 July by the end of July a relatively weak westerly wind dominated (Fig. 2) and upwelling did develop along the northern coast of the Gulf. Total phosphorus and nitrogen transport into the surface layer (before upwelling events along the southern coast) was with the surplus of phosphorus as compared with the Redfield ratio of 7.2, about 450 and 400 tonnes correspondingly. The transport of surplus phosphorus is in accordance with our previous model simulations (Zhurbas *et al*. 2008) and field observations (Vahtera *et al*. 2005) in 1999. However, the relatively larger transport of nitrogen needs some explanation. Such an explanation can be based on the fact that stratification of the water column in the Gulf became stronger and, therefore, the phosphacline and the nitracline were located closer to each other and gradients were larger in the thermocline layer in the summer of 2006 than in 1999.

Easterly wind events — wind speed more than 10 m s^{-1} on 3, 13, 23 and 30 August (Fig. 2) — caused intensive upwelling events along the southern coast of the Gulf and brought altogether about 700 tonnes of nitrogen and 650 tonnes of phosphorus into the surface layer, i.e. a slight surplus of nitrogen. The nitrogen surplus is likely related to the changes in vertical nutrient distributions attained by the beginning of the period of upwelling events along the southern coast (*see* Fig. 9). The model simulation showed the dominance of westward flow in the upper 30-m layer along the southern coast in the period 18–30 July accompanied by a shallowing of

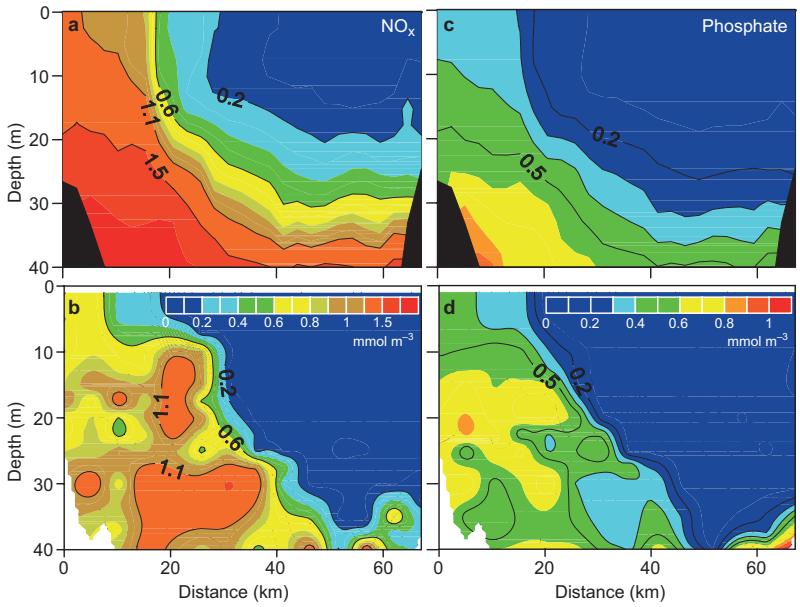

Fig. 7. Comparison of (**a**, **c**) simulated and (**b**, **d**) measured NO_x and PO_4 concentrations along the transect between Tallinn and Helsinki on 8 August. The values on the *x*-axis denote the distance from the southernmost sampling station. Separate colour scales for NO_x and PO_4 concentrations were used.

both the phosphacline and the nitracline. The shallowing was likely caused by the westward flow that would carry nutrient-rich water from deeper layers along the eastward sloping-down isopycnals. Again, taking into account that vertical gradient of NO_x concentration had been initially larger than that of PO_4, the upper boundary of the nitracline (i.e. 0.05 mmol m^{-3} contour) being deeper initially has risen above that of the phosphacline due to a vertical turbulent diffusion which is clearly seen in Fig. 9. This explains a slightly larger simulated transport of nitrogen than of phosphorus into the surface layer by upwelling events along the southern coast of the Gulf in 2006 (Fig. 8). Lips *et al*. (2009) also estimated from field measurements that about equal amounts of nitrogen and phosphorus were transported by upwelling into the surface layer.

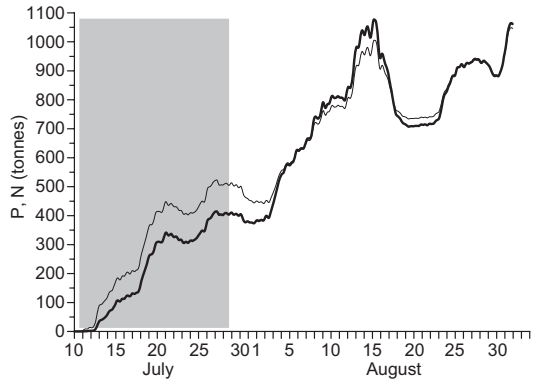

Fig. 8. Temporal course of total content of phosphorus (thin line) and nitrogen (bold line) introduced to the upper 10-m layer due to upwelling events along the northern (shaded area) and southern coasts during the simulation period in the Gulf of Finland.

In order to evaluate how much the lack of nutrient consumption in the model had influenced the above results we compared the changes of nutrient concentrations in the upper layer (0–25 m) for the period of 11–25 July estimated from the model with the measurements along the transect Tallinn–Helsinki. The changes in average concentrations were overestimated by the model only by < 0.02 mmol m^{-3} for PO_4 and < 0.12 mmol m^{-3} for NO_x, which is an order of magnitude less than the observed and calculated increase of nutrient concentrations in the upper layer during the upwelling events in August 2006. It shows that the estimates of total nutrient input to the surface layer of the Gulf produced by a series of strong upwelling events was not biased remarkably by neglecting the nutrient consumption.

A rapid decrease of total nutrient content as a response to a fast change of the wind regime was an expected result. Due to the transient SW wind, favourable for downwelling along the southern coast, on 18 August (Fig. 2), the intensity of upwelling weakened and a decline

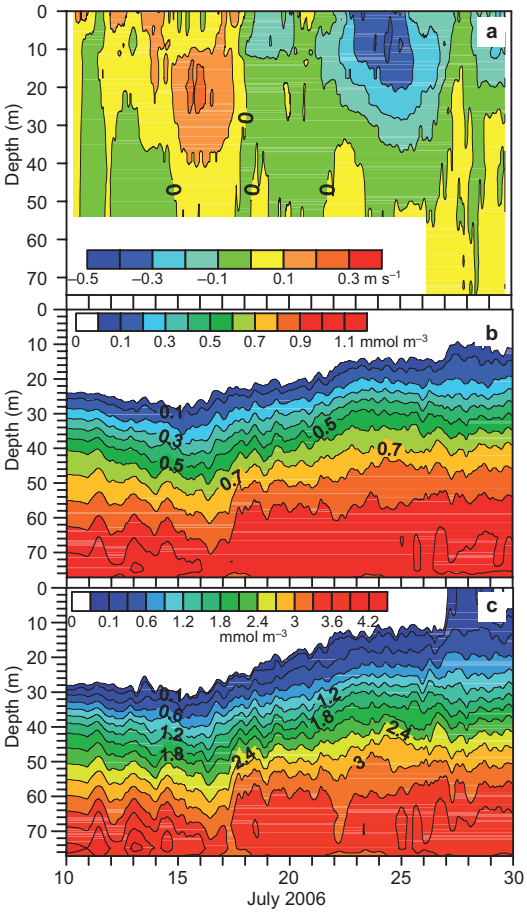

Fig. 9. Temporal course of vertical distribution of (**a**) the *u* component of velocity, (**b**) phosphate, and (**c**) NO_x concentrations at location A (Fig. 1).

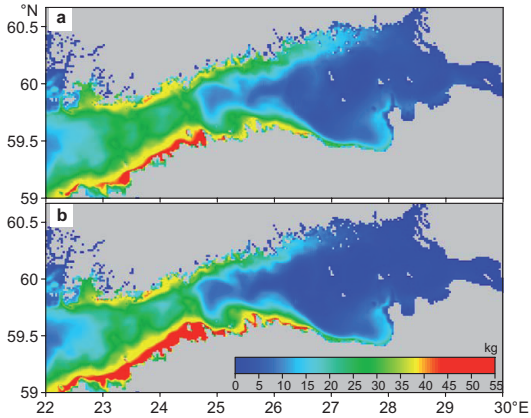

Fig. 10. Maps of mean (**a**) phosphorus and (**b**) nitrogen contents (kg) in the upper 10-m water column with cross section area of 0.5 × 0.5 nautical miles.

of isopycnal surfaces caused a decrease of phosphorus and nitrogen content in the surface layer by 250 and 400 tonnes, respectively. The total amounts of phosphorus and nitrogen transported by upwelling events into the surface layer during July–August was the same (about 1100 tonnes), i.e. with a clear excess of phosphorus (N:P = 1) as compared with the Redfield ratio of 7.2. The clear excess of phosphorus in the upwelled water allows us to suggest that a large part of phosphorus might be utilized by nitrogen-fixing cyanobacteria due to nitrogen limitation of other phytoplankton groups (e.g. Kangro *et al*. 2007). The estimated averaged external bioavailable phosphorus load in the Gulf is about 380 tonnes per month (e.g. Zhurbas *et al*. 2008), which is rather an overestimation due to low river runoff during late summer (Richter and Ebel 2006). Thus, an internal phosphorus load caused by the upwelling events in 2006 likely exceeded the external load during summer months. Combining the current results with those of previous simulations (Zhurbas *et al*. 2008, Laanemets *et al*. 2009) and field measurements (Vahtera *et al*. 2005, Lips *et al*. 2009), one may conclude that summer upwelling events transport phosphorus into the surface layer with a clear excess and the amounts are comparable with the external load.

An important aspect is the identification of areas of the largest nutrient input by upwelling events in the Gulf (Fig. 10). The largest inputs of nutrients occurred in the upwelling zones along both coasts. In the eastern part of the open Gulf, the content of upwelled nutrients was low. One can think of two causes for that. Firstly, the simulation period was characterised by wind patterns more favourable for upwelling events in the western and central parts of the Gulf in comparison to the eastern part. However, an analysis of the seven year (2000–2006) satellite SST data also showed less extensive upwelling events in the eastern part of the Gulf (Uiboupin and Laanemets 2009). Furthermore, the filaments predominantly stretched out from the upwelling front along the Finnish coast and in the western part of the Gulf. Secondly, the sea depth is lower and the bottom slope is less steep in the eastern part of the Gulf than in the central and western parts. The effect of bottom topogra-

phy on upwelling-mediated nutrient input was discussed in Laanemets *et al*. (2009). In the narrow western and central parts of the Gulf, where intensive transverse filaments/squirts and eddies are formed (Fig. 5), the averaged phosphorus and nitrogen content was much higher, because in this area upwelled nutrients are more intensively transported from the coastal zone to the open Gulf area.

Conclusions

Comparisons with satellite SST images and *in situ* measurements showed that upwelling events along both coasts of the Gulf, related mesoscale structures and nutrient distributions were reasonably well reproduced by the model.

The average levels of mean kinetic energy per unit volume of mesoscale/eddy fluctuations (EKE), inertial oscillations (IKE) and mean currents (MKE) in the surface layer of the Gulf were estimated as 0.0072, 0.0021 and 0.0015 $m^2\ s^{-2}$, respectively. The EKE was the highest (up to 0.03 $m^2\ s^{-2}$) in the coastal zones of the Gulf where variable wind forcing produced alternating alongshore baroclinic jet currents due to series of upwelling and downwelling events. Likewise, high values of EKE (0.01–0.02 $m^2\ s^{-2}$) were found in the narrowest western and central part of the Gulf, where intensive transverse squirts and eddies were formed. The distribution of IKE was relatively uniform in open waters (0.004 $m^2\ s^{-2}$) and decreased below 0.002 $m^2\ s^{-2}$ in coastal and shallow zones.

Total inputs of phosphorus and nitrogen caused by upwelling events along the northern and southern coasts were characterised by a clear excess of phosphorus; the input of phosphorus was comparable to or even exceeded the external load. In the eastern part of the Gulf nutrient input was relatively low during the whole simulation period. Spatial distributions of nutrients content in the surface layer caused by a sequence of upwelling events showed that the most intensive coastal offshore exchange occurred in the narrow western and central part of the Gulf.

Acknowledgements: We are thankful to anonymous reviewers for constructive recommendations. The work was supported by the Estonian Science Foundation (grants #7467, #7328 and #6752) and the Russian Foundation for Basic Research (Grant #09-05-00479). Estonian Meteorological and Hydrological Institute kindly provided atmospheric forcing data from HIRLAM and Swedish Meteorological and Hydrological Institute provided initial ocean data in the frame of HIROMB cooperation.

References

Alenius P., Nekrasov A. & Myrberg K. 2003. Variability of the baroclinic Rossby radius in the Gulf of Finland. *Cont. Shelf Res*. 23: 563–573.

Bergström S., Alexandersson H., Carlsson B., Fosefsson W., Karlsson K.G. & Westring G. 2001. Climate and hydrology of the Baltic Sea. In: Wulff F., Rahm L. & Larsson P. (eds.), *A system analysis of the Baltic Sea*, Ecological Studies 148, Springer-Verlag, Berlin Heidelberg New York, pp. 75–112.

Blumberg A.F. & Mellor G.L. 1983. Diagnostic and prognostic numerical calculation studies of the South Atlantic Bight. *J. Geophys. Res*. 88: 4579–4592.

Funkquist L. 2001. HIROMB, an operational eddy-resolving model for the Baltic Sea. *Bulletin of the Maritime Institute in Gdansk* XXVIII: 7–16.

Haapala J. 1994. Upwelling and its influence on nutrient concentration in the coastal area of the Hanko Peninsula, entrance to the Gulf of Finland. *Estuarine Coastal Shelf Sci*. 38: 507–521.

Kahru M., Håkansson B. & Rud O. 1995. Distributions of the sea-surface temperature fronts in the Baltic Sea as derived from satellite imagery. *Cont. Self Res*. 15: 663–679.

Kangro K., Olli K., Tamminen T. & Lignell R. 2007. Species-specific responses of a cyanobacteria-dominated phytoplankton community to artificial nutrient limitation: a Baltic Sea coastal mesocosm study. *Mar. Ecol. Prog. Ser*. 336:15–27.

Kononen K., Huttunen M., Hällfors S., Gentien P., Lunven M., Huttula T., Laanemets J., Lilover M., Pavelson J. & Stips A. 2003. Development of a deep chlorophyll maximum of *Heterocapsa triquetra* Ehrenb. at the entrance to the Gulf of Finland. *Limnol. Oceanogr*. 48: 594–607

Kowalewski M. & Ostrowski M. 2005. Coastal up- and downwelling in the southern Baltic. *Oceanologia* 47: 453–475.

Kuuppo P., Tamminen T., Voss M. & Schulte U. 2006. Nitrogenous discharges to the eastern Gulf of Finland, the Baltic Sea: Elemental flows, stable isotope signatures, and their estuarine modification. *J. Mar. Syst*. 63: 191–208.

Laanemets J., Kononen K., Pavelson J. & Poutanen E.-L. 2004. Vertical location of seasonal nutriclines in the western Gulf of Finland. *J. Mar. Syst*. 52: 1–13.

Laanemets J., Zhurbas V., Elken J. & Vahtera E. 2009. Dependence of upwelling mediated nutrient transport on wind forcing, bottom topography and stratification in the Gulf of Finland: model experiments. *Boreal Env. Res*.

14: 213–225.

Lehmann A., Lorenz P. & Jacob D. 2004. Modelling the exceptional Baltic Sea inflow events in 2002–2003. *Geophys. Res. Lett.* 31: L21308, doi: 10.1029/2004GL020830.

Lehmann A. & Myrberg K. 2008. Upwelling in the Baltic Sea — a review. *J. Mar. Sys.* 74: S3–S12.

Lehtoranta J. 2003. Dynamics of sediment phosphorus in the brackish Gulf of Finland. *Monogr. Boreal Env. Res.* 24: 1–58.

Lips I., Lips U. & Liblik T. 2009. Consequences of coastal upwelling events on physical and chemical patterns in the central Gulf of Finland (Baltic Sea). *Cont. Shelf Res.* 29: 1836–1847.

Lips U., Lips I., Liblik T. & Elken J. 2008. *Estuarine transport versus vertical movement and mixing of water masses in the Gulf of Finland (Baltic Sea)*. US/EU-Baltic International Symposium, 27–29 May 2008, Tallinn. *IEEE/OES*, doi:10.1109/BALTIC.2008.4625535.

Männik A. & Merilain M. 2007. Verification of different precipitation forecasts during extended winter-season in Estonia. *HIRLAM Newsletter* 52: 65–70.

Myrberg K. & Andrejev O. 2003. Main upwelling regions in the Baltic Sea — a statistical analysis based on three-dimensional modeling. *Boreal Env. Res.* 8: 97–112.

Myrberg K., Lehmann A., Raudsepp U., Szymelfenig M., Lips I., Lips U., Matciak M., Kowalewski M., Krężel A., Burska D., Szymanek L., Ameryk A., Bielecka L., Bradtke K., Gałkowska A., Gromisz S., Jędrasik J., Kaluźny M., Kozłowski L., Krajewska-Sołtys A., Ołdakowski B., Ostrowski M., Zalewski M., Andrejev O., Suomi I., Zhurbas V., Kauppinen O.-K., Soosaar E., Laanemets J., Uiboupin R., Talpsepp L., Golenko M., Golenko N. & Vahtera E. 2008. Upwelling events, coastal offshore exchange, links to biogeochemical processes — highlights from the Baltic Sea Science Conference, March 19–22, 2007 at Rostock University. *Oceanologia* 50: 95–113.

Richter K.-G. & Ebel M. 2006. Analysis of runoff for the Baltic Sea basin with an integrated atmosperhic-oceanic-hydrology model. *Advances in Geosciences* 9: 31–37.

Seifert T. & Kayser B. 1995. A high resolution spherical grid topography of the Baltic Sea. *Meereswissenschaftliche Berichte* 9: 72–88.

Soomere T. & Keevallik S. 2003. Directional and extreme wind properties in the Gulf of Finland. *Proc. Estonian Acad. Sci. Eng.* 9: 73–90.

Suursaar Ü. & Aps R. 2007. Spatio-temporal variations in hydrophysical and chemical parameters during a major upwelling event off the southern coast of the Gulf of Finland in summer 2006. *Oceanologia* 49: 209–229.

Tilstone G.H., Míguez B.M., Figueiras F.G. & Fermín E.G. 2000. Diatom dynamics in a coastal ecosystem affected by upwelling: coupling between species succession, circulation and biogeochemical processes. *Mar. Ecol. Prog. Ser.* 205: 23–41.

Vahtera E., Laanemets J., Pavelson J., Huttonen M. & Kononen K. 2005. Effect of upwelling on the pelagic environment and bloom-forming cyanobacteria in the western Gulf of Finland, Baltic Sea. *J. Mar. Sys.* 58: 67–82.

Uiboupin R. & Laanemets J. 2009. Upwelling characteristics derived from satellite sea surface temperature data in the Gulf of Finland, Baltic Sea. *Boreal Env. Res.* 14: 297–304.

Zhurbas V.M., Laanemets J. & Vahtera E. 2008. Modeling of the mesoscale structure of coupled upwelling/downwelling events and the related input of nutrients to the upper mixed layer in the Gulf of Finland, Baltic Sea. *J. Geophys. Res.* 113: C05004, doi: 10.1029/2007JC004280.

Zhurbas V., Oh I. & Park T. 2006. Formation and decay of a longshore baroclinic jet associated with transient coastal upwelling and downwelling: a numerical study with applications to the Baltic Sea. *J. Geophys. Res.* 111: C04014, doi: 10.1029/2005JC003079.